Backstepping Stabilization of the Linearized *Saint-Venant-Exner* Model: Part I – State feedback

Ababacar Diagne, Mamadou Diagne, Shuxia Tang and Miroslav Krstic

Abstract— Using the backstepping design, we achieve exponential stabilization of the coupled Saint-Venant-Exner (SVE) PDE model of water dynamics in a sediment-filled canal with arbitrary values of canal bottom slope, friction, porosity, and water-sediment interaction under subcritical or supercritical flow regime. This model consists of two rightward and one leftward convecting transport Partial Differential Equations (PDEs). A single boundary input control (with actuation located only at downstream) strategy is employed and the backstepping approach developed for the first order linear hyperbolic PDEs is used. A full state feedback controller is designed, which guarantees the exponential stability of the closed-loop control system.

I. Introduction

Balance laws are the key point for modeling complex physical systems that involve fluid mechanics, reactions, heat and mass transfer phenomena. In fluid mechanics, fundamental balance equations expressing the conservation of certain quantities, such as the energy, the mass or the momentum in physical processes, lead to spatio-temporal differential equations that express transport or diffusion phenomena. Such equations are the starting point for the design of various controllers that ensure the stability and operability of many engineering applications. Among those applications, we are interested in the stabilization of the hyperbolic SVE PDEs describing the flow and the bed evolutions in an open channel [4], [6]. To the best of the authors' knowledge, there are only a few results on the stabilization of SVE model in the existing literatures.

Several strategies have been developed to control the flow dynamics in irrigation canals during the last decades. We refer the reader to [10] in which the classification of control problems and related methodologies is fairly addressed. Basically, the main purpose is the regulation of the water level at a desired height by adjusting the opening of the gates, as boundary actuators, at the ends of the channel. For instance, the synthesis of LQ controller can be found in [15], whereas [9] and [11] have studied an H_∞ control approach. Through semigroup approach, [16] proposed an integral output feedback controller using a linearized PDE model around a steady state. Lyapunov analysis is investigated in [12], and multi-models approach with a stability analysis based on Linear Matrix Inequality (*LMI*) is presented in

Ababacar Diagne is with Division of Scientific Computing, Department of Information Technology, Uppsala University, Box 337, 75105 Uppsala, Sweden `ababacar.diagne@it.uu.se`

Mamadou Diagne, Shuxia Tang and Miroslav Krstic are with the Department of Mechanical & Aerospace Engineering, University of California, San Diego, La Jolla, CA 92093-0411 `mdiagne@ucsd.edu`, `sht015@ucsd.edu` and `krstic@ucsd.edu`

[13]. Recently, explicit boundary dissipative conditions are derived in [4] for the exponential stability in L^2-norm of one-dimensional linear hyperbolic systems of balance laws.

Recently, the backstepping method was introduced for the feedback stabilization of various classes of PDEs [3], [8]. The key idea of this approach is the construction of suitable Volterra integral transformations that map the original system into a so-called "target system", which is exponentially stable. The kernel functions of the transformations are required to satisfy some PDEs, and the solutions can be then used as gains of the controllers. The invertibility of the transformations ensures the exponential stability of the closed-loop control systems. One can refer to [2], [8], [14], [1] for further applications of this technique to other classes of systems including nonlinear PDEs.

Using the backstepping design, we achieve exponential stabilization of the coupled Saint-Venant-Exner (SVE) PDE model [4] of water dynamics in a sediment-filled canal with arbitrary values of canal bottom slope, friction, porosity, and water-sediment interaction. A single boundary input control strategy (with actuation located only at downstream) is adopted and the backstepping approach is developed in [3]. Under the subcritical or supercritical flow regime, the studied SVE model consists of two rightward and one leftward convecting transport PDEs.

This paper is organized as follows. In the next Section, the nonlinear SVE model is formulated based on its physical description, and a linearized version around a steady state is presented. Section III is dedicated to the backstepping transformation between the linearized model and a suitable exponentially stable target system. Then, with the solutions to the gain kernel PDEs of the Volterra transformation, a full state controller is computed. Numerical simulations are provided in Section IV Finally in Section V, a conclusion is presented and some perspectives are discussed.

II. The Saint-Venant-Exner model

We consider a pool of a prismatic sloping open channel with a rectangular cross-section, a unit width and a moving bathymetry (because of the sediment transportation). The state variables of the model are: the water depth $H(t,x)$, the water velocity $V(t,x)$ and the bathymetry $B(t,x)$ which is the depth of the sediment layer above the channel bottom, as depicted in Figure 1. The dynamics of the system is described by the coupling of Saint-Venant and Exner equations (see e.g.

[7]):

$$\frac{\partial H}{\partial t} + V\frac{\partial H}{\partial x} + H\frac{\partial V}{\partial x} = 0 \tag{1a}$$

$$\frac{\partial V}{\partial t} + V\frac{\partial V}{\partial x} + g\frac{\partial H}{\partial x} + g\frac{\partial B}{\partial x} = gS_b - C_f\frac{V^2}{H} \tag{1b}$$

$$\frac{\partial B}{\partial t} + aV^2\frac{\partial V}{\partial x} = 0. \tag{1c}$$

In these equations, g is the gravity constant, S_b is the bottom slope of the channel and C_f is a friction coefficient. The coefficient a (cf [7]) is a parameter that encompasses the porosity and viscosity effects on the sediment dynamics, which is expressed as

$$a = \frac{3A_g}{1 - p_g},$$

where p_g is the porosity parameter and A_g is the coefficient to control the interaction between the bed and the water flow.
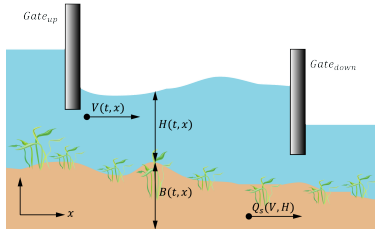

Fig. 1. A sketch of the channel.

A. Steady-state and Linearization

A *steady-state* is a constant state $(H^*, V^*, B^*)^T$ which satisfies the relation $gS_bH^* = C_fV^{*2}$.

In order to linearize the model, we define the deviation of the state $\left(H(t,x), V(t,x), B(t,x)\right)^T$ with respect to the steady-state as

$$\begin{pmatrix} h(x,t) \\ u(x,t) \\ b(x,t) \end{pmatrix} = \begin{pmatrix} H(x,t) - H^* \\ V(x,t) - V^* \\ B(x,t) - B^* \end{pmatrix}.$$

Then the linearized system of the SVE model (1) around the steady-state is

$$\frac{\partial h}{\partial t} + V^*\frac{\partial h}{\partial x} + H^*\frac{\partial u}{\partial x} = 0 \tag{2a}$$

$$\frac{\partial u}{\partial t} + V^*\frac{\partial u}{\partial x} + g\frac{\partial h}{\partial x} + g\frac{\partial b}{\partial x} = C_f\frac{V^{*2}}{H^{*2}}h - 2C_f\frac{V^*}{H^*}u \tag{2b}$$

$$\frac{\partial b}{\partial t} + aV^{*2}\frac{\partial u}{\partial x} = 0. \tag{2c}$$

B. Characteristic (Riemann) coordinates

In the matrix form, the linearized model (2) can be written as

$$\frac{\partial W}{\partial t} + A(W^*)\frac{\partial W}{\partial x} = B(W^*)W, \tag{3}$$

where

$$W = \begin{pmatrix} h \\ u \\ b \end{pmatrix}, \quad A(W^*) = \begin{pmatrix} V^* & H^* & 0 \\ g & V^* & g \\ 0 & aV^{*2} & 0 \end{pmatrix},$$

$$B(W^*) = \begin{pmatrix} 0 & 0 & 0 \\ C_f\frac{V^{*2}}{H^{*2}} & -2C_f\frac{V^*}{H^*} & 0 \\ 0 & 0 & 0 \end{pmatrix}.$$

Exact, but rather complicated expressions of the eigenvalues of $A(W^*)$ can be obtained by using the *Cardano-Vieta* method, see [7]. Once the eigenvalues λ_i of the matrix $A(W^*)$ are obtained, the corresponding left eigenvectors can be computed as

$$L_k = \frac{1}{(\lambda_k - \lambda_i)(\lambda_k - \lambda_j)} \begin{pmatrix} (V^* - \lambda_i)(V^* - \lambda_j) + gH^* \\ H^*\lambda_k \\ gH^* \end{pmatrix},$$

$$\text{for } k \neq i \neq j \in \{1,2,3\}. \tag{4}$$

We multiply (3) by L_k^T in order to rewrite the model in terms of the characteristic coordinates ψ_k ($k = 1, 2, 3$). Then we obtain

$$\frac{\partial \Phi_k}{\partial t} + \lambda_k\frac{\partial \Phi_k}{\partial x} = L_k^T BW, \text{ for } k = 1,2,3, \tag{5}$$

where

$$\Phi_k = \frac{1}{(\lambda_k - \lambda_i)(\lambda_k - \lambda_j)} \left[\left((V^* - \lambda_i)(V^* - \lambda_j) + gH^*\right)h + H^*\lambda_k u + gH^* b \right]. \tag{6}$$

For the sake of simplicity, we introduce this notation:

$$r_k = C_f\frac{V^*}{H^*}\frac{\lambda_k}{(\lambda_k - \lambda_i)(\lambda_k - \lambda_j)}.$$

Some computations yield the following expression for (5):

$$\frac{\partial \xi_k}{\partial t} + \lambda_k\frac{\partial \xi_k}{\partial x} + \sum_{s=1}^{3}(2\lambda_s - 3V^*)r_s\xi_s = 0, \text{ for } k = 1,2,3, \tag{7}$$

where the characteristic coordinates are now defined as

$$\xi_k = \frac{1}{r_k}\Phi_k. \tag{8}$$

From (7), the linearized model (5) in characteristic form can be written as

$$\frac{\partial \xi}{\partial t} + \Lambda\frac{\partial \xi}{\partial x} - M\xi = 0, \tag{9}$$

where

$$\xi = (\xi_1, \xi_2, \xi_3)^T, \quad \Lambda = diag(\lambda_1, \lambda_2, \lambda_3),$$

and

$$M = \begin{pmatrix} \alpha_1 & \alpha_2 & \alpha_3 \\ \alpha_1 & \alpha_2 & \alpha_3 \\ \alpha_1 & \alpha_2 & \alpha_3 \end{pmatrix}, \text{ where } \alpha_k = \left(3V^* - 2\lambda_k\right)r_k. \tag{10}$$

The dimensionless Froude number is defined as

$$Fr = \frac{V^*}{\sqrt{gH*}}. \tag{11}$$

From [7], the three eigenvalues of the matrix A are such that for a subcritical flow regime $(Fr < 1)$,

$$\lambda_1 < 0 < \lambda_2 < \lambda_3; \tag{12}$$

and for a supercritical one $(Fr > 1)$,

$$\lambda_2 < 0 < \lambda_1 < \lambda_3, \tag{13}$$

with λ_1 and λ_3 being the characteristic velocities of the water flow and λ_2 being the characteristic velocity of the sediment motion.

Hereafter, we consider the case where the flow regime is subcritical and adopt the following notations: $v(t,x) = \xi_1(t,x)$, $u_1(t,x) = \xi_2(t,x)$, $u_2(t,x) = \xi_3(t,x)$ and coefficients (characteristic velocities) $\mu = -\lambda_1$, $\gamma_1 = \lambda_2$ and $\gamma_2 = \lambda_3$. We introduce also the vector $\boldsymbol{u} = (u_1, u_2)^T$, the coefficients $\eta_j = \alpha_{j+1}$ for $j = 1, 2$ and the matrix

$$\boldsymbol{\sigma} = \begin{pmatrix} \alpha_2 & \alpha_3 \\ \alpha_2 & \alpha_3 \end{pmatrix}. \tag{14}$$

With the new variables, the set of equations (9) is written as:

$$\partial_t u_1 + \gamma_1 \partial_x u_1 = \sigma_{11} u_1 + \sigma_{12} u_2 + \alpha_1 v \tag{15a}$$
$$\partial_t u_2 + \gamma_2 \partial_x u_2 = \sigma_{21} u_1 + \sigma_{22} u_2 + \alpha_1 v \tag{15b}$$
$$\partial_t v - \mu \partial_x v = \eta_1 u_1 + \eta_2 u_2 + \alpha_1 v. \tag{15c}$$

Introduce the variable

$$w(t,x) = v(t,x) \exp\left(-\frac{\alpha_1}{\mu} x\right),$$

then the system (15) is transformed into

$$\partial_t u_1 + \gamma_1 \partial_x u_1 = \sigma_{11} u_1 + \sigma_{12} u_2$$
$$+ \alpha_1 \exp\left(\frac{\alpha_1}{\mu} x\right) w \tag{16a}$$
$$\partial_t u_2 + \gamma_2 \partial_x u_2 = \sigma_{21} u_1 + \sigma_{22} u_2$$
$$+ \alpha_1 \exp\left(\frac{\alpha_1}{\mu} x\right) w \tag{16b}$$
$$\partial_t w - \mu \partial_x w = \eta_1 \exp\left(\frac{\alpha_1}{\mu} x\right) u_1$$
$$+ \eta_2 \exp\left(\frac{\alpha_1}{\mu} x\right) u_2. \tag{16c}$$

We rewrite this system as:

$$\partial_t u_1 + \gamma_1 \partial_x u_1 = \sigma_{11} u_1 + \sigma_{12} u_2 + \alpha(x) w \tag{17a}$$
$$\partial_t u_2 + \gamma_2 \partial_x u_2 = \sigma_{21} u_1 + \sigma_{22} u_2 + \alpha(x) w \tag{17b}$$
$$\partial_t w - \mu \partial_x w = \theta_1(x) u_1 + \theta_2(x) u_2 \tag{17c}$$

with $\alpha(x) = \alpha_1 \exp\left(\frac{\alpha_1}{\mu} x\right)$ and $\theta_j(x) = \alpha_{j+1} \exp\left(\frac{\alpha_1}{\mu} x\right)$ for $j = 1, 2$.

To close the writing of the system (17), we enclose to it the following boundary and initial conditions:

$$u_i(t,0) = q_i w(t,0) \quad \text{for } i = 1, 2, \tag{18a}$$
$$w(t,1) = \rho_1 u_1(t,1) + \rho_2 u_2(t,1) + U(t), \tag{18b}$$
$$w(0,x) = w^0(x), \ u_i(0,x) = u_i^0(x) \quad \text{for } i = 1, 2. \tag{18c}$$

u_1, u_2 and w are the distributed states, and $U(t)$ is the control input. The measured output is given by: $w(t,0) = y(t)$.

III. FULL STATE CONTROLLER DESIGN

A. Backstepping transformation and target system

Consider the following backstepping transformation

$$\psi_i(t,x) = u_i(t,x) \text{ for } i = 1, 2 \tag{19}$$
$$\chi(t,x) = w(t,x) - \int_0^x k_1(x,\xi) u_1(t,\xi) \, d\xi$$
$$- \int_0^x k_2(x,\xi) u_2(t,\xi) \, d\xi - \int_0^x k_3(x,\xi) w(t,\xi) \, d\xi. \tag{20}$$

We now seek a sufficient condition on the functions k_i such that the transformation (19)-(20) maps the system (17)-(18) to the target system

$$\partial_t \psi_1 + \gamma_1 \partial_x \psi_1 = \sigma_{11} \psi_1 + \sigma_{12} \psi_2 + \alpha(x) \chi$$
$$+ \int_0^x c_{11}(x,\xi) \psi_1(t,\xi) \, d\xi$$
$$+ \int_0^x c_{12}(x,\xi) \psi_2(t,\xi) \, d\xi$$
$$+ \int_0^x \kappa_1(x,\xi) \chi(t,\xi) \, d\xi \tag{21a}$$
$$\partial_t \psi_2 + \gamma_2 \partial_x \psi_2 = \sigma_{21} \psi_1 + \sigma_{22} \psi_2 + \alpha(x) \chi$$
$$+ \int_0^x c_{21}(x,\xi) \psi_1(t,\xi) \, d\xi$$
$$+ \int_0^x c_{22}(x,\xi) \psi_2(t,\xi) \, d\xi$$
$$+ \int_0^x \kappa_2(x,\xi) \chi(t,\xi) \, d\xi \tag{21b}$$
$$\partial_t \chi - \mu \partial_x \chi = 0 \tag{21c}$$

with the following boundary conditions:

$$\psi_i(t,0) = q_i \chi(t,0) \text{ for } i = 1, 2 \text{ and } \chi(t,1) = 0. \tag{22}$$

Here, $c_{ij}(\cdot)$ and $\kappa_i(\cdot)$ are functions to be determined on the triangular domain

$$\mathbb{T} = \left\{ (x,\xi) \in \mathbb{R}^2 \mid 0 \leq \xi \leq x \leq 1 \right\}.$$

The system (21)-(22) is designed as a copy of the original plant with the coupling term in (17c) removed. As will be shown later, the new terms in (21a) and (21b) are necessary for the design but they will not affect the stability.

A sufficient condition for the transformation (19)-(20) to map the original system (17) into the target system (21) is that the kernels k_i satisfy the following system of first order hyperbolic PDEs:

$$\mu \partial_x k_1(x,\xi) - \gamma_1 \partial_\xi k_1(x,\xi)$$
$$= \sigma_{11} k_1(x,\xi) + \sigma_{21} k_2(x,\xi) + \theta_1(\xi) k_3(x,\xi) \tag{23a}$$
$$\mu \partial_x k_2(x,\xi) - \gamma_2 \partial_\xi k_2(x,\xi)$$
$$= \sigma_{12} k_1(x,\xi) + \sigma_{22} k_2(x,\xi) + \theta_2(\xi) k_3(x,\xi) \tag{23b}$$
$$\mu \partial_x k_3(x,\xi) + \mu \partial_\xi k_3(x,\xi)$$
$$= \alpha(\xi) k_1(x,\xi) + \alpha(\xi) k_2(x,\xi) \tag{23c}$$

with the following boundary conditions:

$$k_1(x,x) = -\frac{\theta_1(x)}{\gamma_1 + \mu}, \quad k_2(x,x) = -\frac{\theta_2(x)}{\gamma_2 + \mu}, \tag{24a}$$
$$\mu k_3(x,0) = q_1 \gamma_1 k_1(x,0) + q_2 \gamma_2 k_2(x,0). \tag{24b}$$

The existence, uniqueness and continuity of the solutions to the system (23) with boundary conditions (24) are assessed by Theorem 5.3 in [3].

Besides, plugging (19)-(20) into (21) and using (17)-(18), we can see that the coefficients κ_i can be chosen to satisfy the following integral equation for $i = 1, 2$

$$\kappa_i(x,\xi) = \alpha(x)k_3(x,\xi) + \int_\xi^x \kappa_i(x,s)k_3(s,\xi)\,ds, \quad (25)$$

and the coefficients c_{ij} can be chosen such that

$$c_{ij}(x,\xi) = \alpha(x)k_j(x,\xi) + \int_\xi^x \kappa_i(x,s)k_j(s,\xi)\,ds$$
$$\text{for } i, j = 1, 2 \quad (26)$$

under the fact that the k_i exist and are sufficiently smooth.

B. Inverse transformation and control law

To ensure that the target system and the closed-loop system have equivalent stability properties, the transformation (19)-(20) has to be invertible. Since $\psi_i = u_i$, for $i = 1, 2$, the transformation (20) can be rewritten as

$$\chi(t,x) + \int_0^x k_1(x,\xi)\psi_1(t,\xi)\,d\xi + \int_0^x k_2(x,\xi)\psi_2(t,\xi)\,d\xi$$
$$= w(t,x) - \int_0^x k_3(x,\xi)w(t,\xi)\,d\xi. \quad (27)$$

Let us define

$$\Gamma(t,x) = \chi(t,x) + \int_0^x k_1(x,\xi)\psi_1(t,\xi)\,d\xi$$
$$+ \int_0^x k_2(x,\xi)\psi_2(t,\xi)\,d\xi. \quad (28)$$

Since k_3 is continuous by Theorem 5.3 in [3], there exists a unique continuous inverse kernel l_3 defined on $\mathbb{T}$, such that

$$w(t,x) = \Gamma(t,x) + \int_0^x l_3(x,\xi)\Gamma(t,\xi)\,d\xi, \quad (29)$$

Since $\psi_i = u_i$, for $i = 1, 2$, we could get the following relation from the first two equalities of (17) and (21):

$$\alpha(x)w = \alpha(x)\chi + \int_0^x c_{11}(x,\xi)\psi_1(t,\xi)\,d\xi$$
$$+ \int_0^x c_{12}(x,\xi)\psi_2(t,\xi)\,d\xi + \int_0^x \kappa_1(x,\xi)\chi(t,\xi)\,d\xi. \quad (30)$$

Thus, we could write the following inverse transformation

$$w(t,x) = \chi(t,x) + \int_0^x l_1(x,\xi)\psi_1(t,\xi)\,d\xi$$
$$+ \int_0^x l_2(x,\xi)\psi_2(t,\xi)\,d\xi + \int_0^x l_3(x,\xi)\chi(t,\xi)\,d\xi, \quad (31)$$

where for $i = 1, 2$,

$$l_i(x,\xi) = k_i(t,\xi) + \int_\xi^x k_i(x,\xi)l_3(\xi,s)\,ds. \quad (32)$$

Thus, the control law $U(t)$ can be obtained by plugging the transformation (20) into (17). Readily, $\chi(t,1) = 0$ implies that

$$U(t) = -\rho_1 u_1(t,1) - \rho_2 u_2(t,1) + \int_0^1 \Big[k_1(1,\xi)u_1(x,\xi)$$
$$+ k_2(1,\xi)u_2(x,\xi) + k_3(1,\xi)w(1,\xi) \Big]\,d\xi. \quad (33)$$

The k_i in the integral term designate the kernel functions and satisfy the system (23)-(24).

Remark 1: Let us mention that in the case where the flow regime is supercritical, namely, $(F_r > 1)$, the following changes of variable will be considered regarding on the characteristics, $v(t,x) = \xi_2(t,x)$, $u_1(t,x) = \xi_1(t,x)$, $u_2(t,x) = \xi_3(t,x)$ and coefficients $\lambda_2 = -\mu$, $\lambda_1 = \gamma_1$ and $\lambda_3 = \gamma_2$.

C. Stability of the target system and the closed-loop control system

We first prove exponential stability of the target system (21)-(22).

Lemma 1: For any given initial condition $(\psi_1^0, \ \psi_2^0, \ \chi^0)^T \in \big(\mathscr{L}^2([0,1])\big)^3$ and under the assumption that $c_{ij}, \ \kappa_i \in \mathscr{C}(\mathbb{T})$, the equilibrium $(\psi_1, \ \psi_2, \ \chi)^T = (0, \ 0, \ 0)^T$ of the target system (21)-(22) is $\mathscr{L}^2$-exponentially stable.

Proof 1: The stability proof is based on the time differentiation of the following Lyapunov function:

$$V_1(t) = \int_0^1 a_1 e^{-\delta_1 x}\left(\frac{\psi_1^2(t,x)}{\gamma_1} + \frac{\psi_2^2(t,x)}{\gamma_2} \right)dx$$
$$+ \int_0^1 \frac{1+x}{\mu}\chi^2(t,x)dx, \quad (34)$$

where a_1 and δ_1 are strictly positive parameters to be determined.

Take $\varepsilon = \min\{\gamma_1, \gamma_2\} > 0$. Assume that for $M > 0$, we have

$$\|\boldsymbol{\sigma}\|, \ \|\boldsymbol{\alpha}(x)\|, \|\boldsymbol{C}(x,\xi)\|, \ \|K(x,\xi)\| \leq M,$$
$$\forall x \in [0,1], \xi \in [0,x], \quad (35)$$

where the matrix/vector norms $\|\cdot\|$ are compatible with the other corresponding matrix/vector norms.

$$\Psi(t,x) = \begin{pmatrix} \psi_1(t,x) \\ \psi_2(t,x) \end{pmatrix}, \ \boldsymbol{\alpha}(x) = \begin{pmatrix} \alpha(x) \\ \alpha(x) \end{pmatrix} \quad (36)$$

$$K(x,\xi) = \begin{pmatrix} \kappa_1(x,\xi) \\ \kappa_2(x,\xi) \end{pmatrix}, \Gamma_{inv} = \begin{pmatrix} \frac{1}{\gamma_1} & 0 \\ 0 & \frac{1}{\gamma_2} \end{pmatrix} \quad (37)$$

$$\boldsymbol{C}(x,\xi) = \begin{pmatrix} c_{11}(x,\xi) & c_{12}(x,\xi) \\ c_{21}(x,\xi) & c_{22}(x,\xi) \end{pmatrix}. \quad (38)$$

Then, differentiating this function with respect to time, taking into account of the target system (21)-(22), integrating by parts and applying Young's inequality at different steps, we obtain the following inequality:

$$\dot{V}_1(t) \leq \left(a_1 \sum_{i=1}^2 q_i^2 - 1 \right)\chi^2(t,0)$$
$$- \int_0^1 \left(1 - a_1(1 + \frac{1}{\delta_1})e^{-\delta_1 x} \right)\chi^2(t,x)\,dx$$
$$- a_1 \int_0^1 e^{-\delta_1 x}\Psi^T(t,x)P(x)\Psi(t,x)\,dx, \quad (39)$$

where,

$$P(x) = \left(\delta_1 - 2\frac{M}{\varepsilon} - \frac{M}{\varepsilon}x - 2\left(\frac{M}{\varepsilon}\right)^2 - \frac{M}{\delta_1 \varepsilon} \right)I_2 - 2\Gamma_{inv}\boldsymbol{\sigma}, \quad (40)$$

First, we choose the tuning parameter $\delta_1 > 0$ sufficiently large so that the matrix $P(x), x \in [0,1]$ is positive definite. Then, by choosing

$$0 < a_1 < \min \left\{ \frac{1}{\sum\limits_{i=1}^{2} q_i^2}, \frac{\delta_1}{\delta_1 + 1} \right\}, \tag{41}$$

we could derive exponential stability of the target system. Then, from the continuity and invertibility of the backstepping transformation (19)-(20), we could derive equivalence between the original system (17) (with the boundary and initial conditions (18) and the control law (33) and the target system (21)-(22). Thus, the following theorem is proved.

Theorem 1: Consider the system (17) with the boundary and initial conditions (18) and the control law (33). Then under the assumptions that the initial data are in $\left(\mathscr{L}^2([0,1])\right)^3$, the origin is exponentially stable in the $\mathscr{L}^2$ sense.

Remark 2: Conversely, we can express h, u and b in terms of the characteristic coordinates (6) and (8).

IV. NUMERICAL SIMULATIONS

This section is devoted to the numerical simulations of system (15) subject to the boundary conditions (18) where the state feedback control law $U(t)$ defined in (33). For the implementation of the control, a resolution of the kernel PDE's system (23)-(24) on $\mathbb{T}$ is requested. The initial bottom topography is defined as

$$B(0,x) = 0.4\left(1 + 0.25\exp\left(-\frac{(x-0.5)^2}{0.003}\right)\right),$$

with a gaussian distribution centered at the middle of the domain. The initial water level and its velocity field are computed, respectively as

$$H(0,x) = 2.5 - B(0,x) \quad \text{and} \quad H(0,x)V(0,x) = 10\sin(\pi x).$$

From the physical variables of $H(0,x)$, $V(0,x)$ and $B(0,x)$, the initial data of the characteristic variables v, u_1 and u_2 are derived. All further physical parameters of the physical model are listed in the Appendix. The set point (H^*, V^*, B^*) leads to the following characteristic speed values

$$\lambda_1 = -1.43, \lambda_2 = 0.76 \text{ and } \lambda_3 = 7.42.$$

The coefficients α_i and θ_i and the matrix σ are computed with the help the characteristics values λ_i. Actually, this problem is particularly challenging since all these coefficients do not vanish.

After solving numerically the kernel PDEs (23), the value of the kernel k_1, k_2 and k_3 at $x = 1$ (Fig. 2) are employed for the implementation of the state feedback controller (33).

As depicted in Figure 3 the control input $U(t)$ and the output measurement $y(t)$ at upstream converge fastly to the set point. Clearly, despite the initial amplitude of $U(t)$, this latter one decreases in time and vanishes after $t \geq 4s$. Let us remind that the implementation of $U(t)$ requires a full-state measurement. Moreover, output measurement $y(t)$ shows the
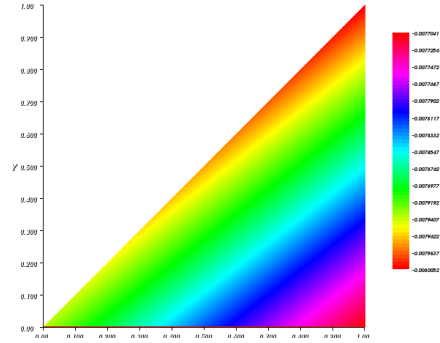

Fig. 2. Numerical solution of the kernel component k_1 on $\mathbb{T}$

same trend with its amplitude decreasing in time and tending to zero after $t \geq 3s$. In figure (4) we plot the evolution in time
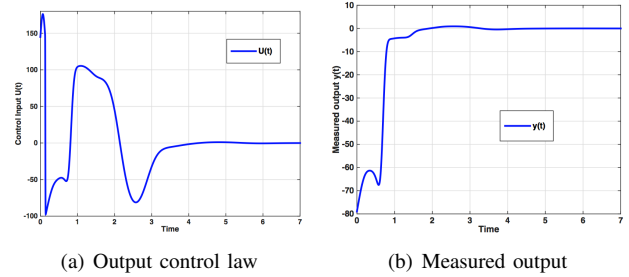

(a) Output control law   (b) Measured output

Fig. 3. Evolution in time of the $U(t)$ and $y(t)$.

of the L^2-norm of the characteristics. As expected from the theoritical part we observe that the norm of the characteristics converge to zero. As a result this shows that the system (17) converges to the zero equilibrium and hence the physical linearized model (2) also converge to (H^*, V^*, B^*).
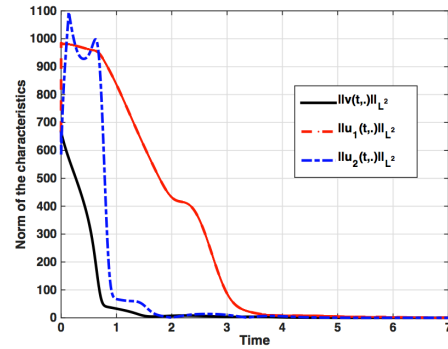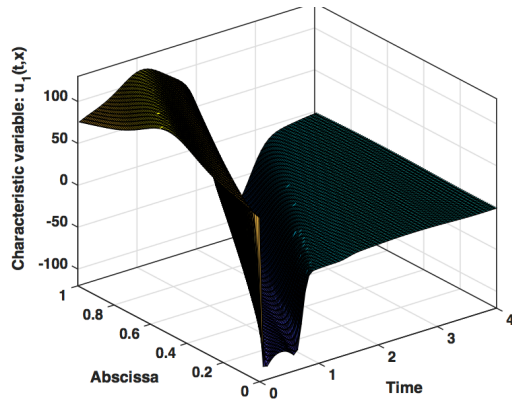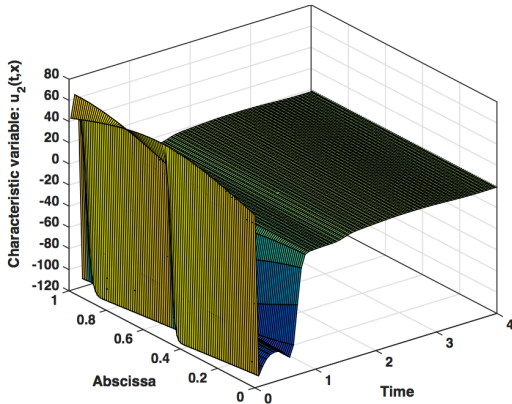

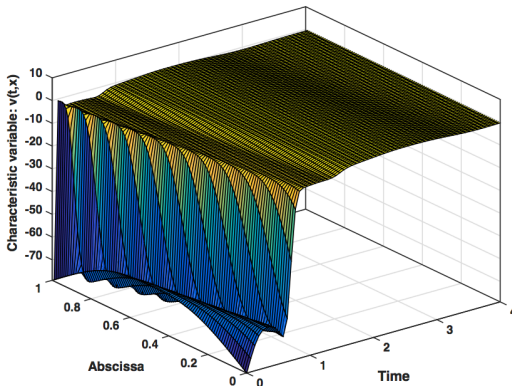Fig. 4. Evolution in time of the norm of the characteristic solution.

Figure 5 describes the space and time dynamics of the plant and is consistent with the numerical results presented above. As time increases, we notice that the perturbation in the overall system decreases and vanishes later. In addition, when comparing Figure 5(a) with Figure 5(c) and 5(b), it is seen that the propagation velocity differs from the characteristic related to the fluid part to the one related to the sediment layers.

(a) Evolution of $u_1(t,x)$

(b) Evolution of $u_2(t,x)$

(c) Evolution of $v(t,x)$

Fig. 5. Behavior in time and space of the characteristic solutions.

V. CONCLUSION

In this paper, the state feedback backstepping control of the linearized SVE equation is presented with an actuator located at the downstream gate of the channel. The designed controller allows to stabilize the SVE system under both supercritical and subcritical flow regime and the qualitative and physical behiavior of the backstepping controller is successfully illustrated in the simulations with the subcritical regime. In the companion paper [5] using the backstepping output feedback control strategy, the supercritical flow regime is simulated.

REFERENCES

[1] P. Bernard and M. Krstic. Adaptive output-feedback stabilization of non-local hyperbolic {PDEs}. *Automatica*, 50(10):2692 – 2699, 2014.
[2] Jean-Michel Coron, Rafael Vazquez, Miroslav Krstic, and Georges Bastin. Local exponential H^2 stabilization of a 2×2 quasilinear hyperbolic system using backstepping. *SIAM Journal on Control and Optimization*, 51(3):2005–2035, 2013.
[3] F. Di Meglio, R. Vazquez, and M. Krstic. Stabilization of a system of coupled first-order hyperbolic linear PDEs with a single boundary input. *IEEE Transactions on Automatic Control*, 58(12):3097–3111, 2013.
[4] Ababacar Diagne, Georges Bastin, and Jean-Michel Coron. Lyapunov exponential stability of 1-d linear hyperbolic systems of balance laws. *Automatica*, 2011.
[5] Ababacar Diagne, Mamadou Diagne, Shuxia Tang, and Miroslav Krstic. Backstepping stabilization of the linearized *Saint-Venant-Exner* model: Part ii – output feedback approach. In *the 2015 CDC conference, under review*, 2015.
[6] Ababacar Diagne and Abdou Sène. Control of shallow water and sediment continuity coupled system. *Mathematics of Control, Signal and Systems (MCSS)*, pages 387–406, 2013.
[7] J. Hudson and P.K. Sweby. Formulations for numerically approximating hyperbolic systems governing sediment transport. *Journal of Scientific Computing*, 19:225–252, 2003.
[8] Miroslav Krstic and Andrey Smyshlyaev. *Boundary control of PDEs: A course on backstepping designs*, volume 16. Siam, 2008.
[9] X. Litrico and Vincent Fromion. H$^\infty$ control of an irrigation canal pool with a mixed control politics. *IEEE Transactions on Control Systems Technology*, 14(1):99–111, 2006.
[10] Pierre olivier Malaterre, David C. Rogers, and Jan Schuurmans. Classification of canal control algorithms. *Journal of Irrigation and Drainage Engineering*, 124(1):3–10, 1998.
[11] P. Pognant-Gros, V. Fromion, and J.P. Baume. Canal controller design : a multivariable approach using h infini. In *Proceedings of the European Control Conference, Portugal*, pages 3398–3403, 2001.
[12] Christophe Prieur and Jonathan de Halleux. Stabilization of a 1-d tank containing a fluid modeled by the shallow water equations. *Systems & Control Letters*, 52(3-4):167–178, 2004.
[13] V. M. Dos Santos, M. Rodrigues, and M. Diagne. A multi-models approach of saint-venants equations : A stability study by lmi. *International Journal of Applied Mathematics and Computer Science*, 22(3):539–550, 2008.
[14] A. Smyshlyaev and M. Krstic. Closed-form boundary state feedbacks for a class of 1-d partial integro-differential equations. *Automatic Control, IEEE Transactions on*, 49(12):2185–2202, Dec 2004.
[15] E. Weyer. LQ control of an irrigation channel. In *Proceedings of the 42nd IEEE Conference on Decision and Control*, volume 1, pages 750–755, 2003.
[16] C. Z. Xu and G. Sallet. Proportional and integral regulation of irrigation canal systems governed by the saint-venant equation. In *In Proceedings of the 14th world congress IFAC,Beijing*, pages 147–152, 1999.